frontiers
in Marine Science

Real-Time Thickness Measurement of Marine Oil Spill by Fiber-Optic Surface Plasmon Resonance Sensors

Huiting Yin[1], Shaohuang Chen[1], Renliang Huang[2,3], Heng Chang[1], Jiayue Liu[3]*, Wei Qi[1,4], Zhimin He[1] and Rongxin Su[1,2,3,4]*

[1] State Key Laboratory of Chemical Engineering, Tianjin Key Laboratory of Membrane Science and Desalination Technology, School of Chemical Engineering and Technology, Tianjin University, Tianjin, China, [2] Zhejiang Institute of Tianjin University, Ningbo, China, [3] School of Marine Science and Technology, Tianjin University, Tianjin, China, [4] Collaborative Innovation Center of Chemical Science and Engineering (Tianjin), Tianjin, China

Rapid detection of marine oil spills is becoming increasingly critical in the face of frequent marine oil spills. Oil slick thickness measurement is critical in the hazard assessment of such oil leaks. As surface plasmon resonance (SPR) sensors are sensitive to slight changes in refractive index, they can monitor offshore oil spills arising from significant differences in the refractive index between oil and water. This study presents a gold-film fiber-optic surface plasmon resonance (FOSPR) sensor prepared by polydopamine accelerated wet chemical plating for rapid and real-time measurement of oil slick thickness. We examined oil thickness detection at two interfaces, namely, water-oil and air-oil. Detection sensitivity of −1.373%/mm is obtained at the water-oil interface in the thickness range of 0–5 mm; detection sensitivity of −2.742%/mm is obtained at the air-oil interface in the thickness range of 0–10 mm. Temperature and salinity present negligible effects on the oil slick thickness measurement. The fabricated FOSPR sensor has the ability to detect the presence of oil as well as quantify the oil thickness. It has favorable repeatability and reusability, demonstrating the significant potential for use in the estimation of marine oil slick thickness.

Keywords: oil spill, optical fiber, surface plasmon resonance, thickness, detection

INTRODUCTION

Oil spills have emerged as a major threat to marine ecosystems in recent years, arousing considerable political, environmental, and scientific concern (Beyer et al., 2016; Wan and Chen, 2018; Naz et al., 2021). The large-scale industrial disaster caused by the explosion of the Deepwater Horizon platform of British Petroleum in the Gulf of Mexico resulted in an estimated 200-million-gallon oil spill. Then, severe air contamination was caused by approximately 2 million gallons of dispersant chemicals that were applied to clean the spill (Washburn et al., 2018). The disaster

resulted in adverse health effects and significant damage to the gulf ecosystem (Rotkin-Ellman et al., 2010; Schaum et al., 2010; Leifer et al., 2012). Oil spills are harmful to large areas, including numerous habitats, species, and ecological functions (Beyer et al., 2016). Offshore oil spills share the characteristics of rapid onset, large distribution, and high drift and dispersion dynamics (Peterson et al., 2003).

Due to such broad negative consequences, achieving rapid oil spill emergency response and hazard assessment of ocean oil spills are of great significance (Saleh et al., 2019). Oil slick thickness measurement is directly related to the estimation of oil leak scale and selecting and optimizing oil spill countermeasures (Fingas and Brown, 2014; Sun and Hu, 2019). The detection of slick thickness is also useful to determine the effectiveness of such countermeasures (e.g., *in situ* burning and chemical dispersion) and understand the physical distribution of oil in the sea and its spreading rates (Massaro et al., 2012). Although at an early stage of development, achieving accurate measurement of oil thickness is critical, especially for real-time detection. Some oil thickness measurement methods have been developed, both in the laboratory and in the field (Brown and Fingas, 2003; Fingas, 2018), employing concepts that include near-infrared reflectance, spectral differences, infrared emission, and radar methods-wave damping (Shih and Andrews, 2008; Wettle et al., 2009; Leifer et al., 2012; Li et al., 2012; Lu et al., 2013; De Padova et al., 2017). To date, various sensing technologies have been applied in the measurement of oil slicks on the sea surface and include optical (visible and infrared multispectral and hyperspectral), microwave [synthetic aperture radar (SAR)], side-looking airborne radar (SLAR), microwave radiometer, laser fluorescence, and thermal sensors (Jiang et al., 2018; Guo et al., 2020; Moon and Jung, 2020; Li et al., 2021). Garcia-Pineda et al. (2020) summarized the methods used for the rapid classification of oil types and thickness estimation. Among these, SAR was determined as suitable for large areas and long-distance monitoring at night and in bad weather, with good spatial resolution. Oil spills appear dark in SAR images because sea surface capillaries and short gravity waves can be dampened by oil (Tong et al., 2019). However, the phenomenon of dark areas in SAR images is difficult to clarify as they can also be caused by natural surface films produced by plankton or fish, grease, floating algae, and internal waves. Laser fluorescence sensors also have all-weather characteristics and distinguish oil from other substances by its strong fluorescence characteristics (Bukin et al., 2020). Thermal sensors can detect oil by thermal comparisons generated by the different emissivity of water and oil on the sea surface, which can also indicate its thickness. Jiao et al. (2021) quantified ocean surface oil thickness by using thermal remote sensing, demonstrating the potential of thermal data in providing unique information. Optical sensors have also been successfully used to detect the presence of oil and quantify its volume or thickness (Caillault et al., 2021). In terms of spectral differences, several studies have reported the correlation between slick thickness and specific wavelengths ranging over the visible spectrum. However, researchers have reported different changes in spectral brightness or reflectance as a result of increased thickness and reached contradictory conclusion (Zhan et al., 2010; Ye et al., 2015).
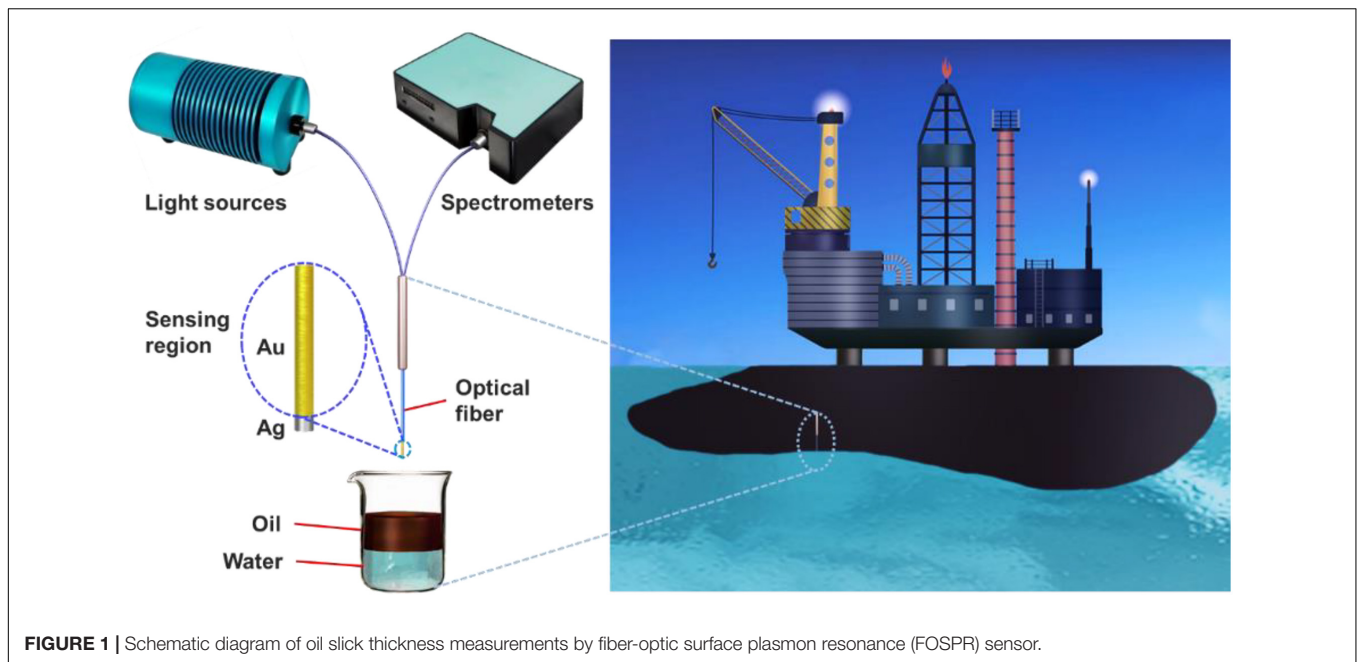
Several fiber-optic sensor structures based on surface plasmon resonance (SPR) have been reported as follows: hetero-core (Liu et al., 2017), U-shaped (Semwal et al., 2016), D-shaped (Patnaik et al., 2015), tapered (Goswami et al., 2016), end-face reflected (Zhao et al., 2017), and unclad/etched sensing structures (Shrivastav et al., 2016). Unclad/etched sensing structures are made by removing the part of the optical fiber cladding and then coating the sensing region on the fiber surface with metal film (using silver, gold, platinum, and other metals) *via* physical evaporation, sputtering, or electroless plating (ELP). ELP is a chemical coating technique based on the chemical reduction of metal ions, which in turn deposits metals on the surface of the substrate. ELP is beneficial in the preparation of fiber-optic SPR sensors as it can overcome physical evaporation or sputtering difficulties when forming uniform films on very thin fiber-optic cylinders. Hoseinian and Bolorizadeh (2019) designed a highly sensitive SPR optical fiber sensor based on a three-strut wagon-wheel structure coated with a gold layer of nano-sized thickness to enhance detection sensitivity. Miliutina et al. (2020) proposed a method to improve surface plasmon fiber sensor sensitivity by grafting gold nanoparticles. Tang et al. (2020) reported a facile method for the fabrication of polydopamine (PDA)/Ag/PDA-based localized SPR sensors based on the strong self-polymerization capability of PDA and the *in situ* growth of Ag nanoparticles for LSPR sensing.

We introduced a novel real-time technique to measure oil slick thickness rapidly and effectively using a gold-film fiber-optic surface plasmon resonance (FOSPR) sensor in this study (**Figure 1**). The sensor is prepared using PDA accelerated wet chemical plating. While most detection methods can measure the thickness of oil on seawater, they fail to detect submarine oil leakages. The terminal reflective FOSPR sensors proposed in this study can achieve detection in the flow cell and immersion situations and eliminate electromagnetic interference in seawater detection (Sharma et al., 2007). The spectral reflectance reduces as the thickness of the oil slick increases, making it possible to use FOSPR sensors to determine oil slick thickness. We examined the effects of salinity and temperature on oil thickness measurement in detail and investigated the repeatability of the sensors. Rapid detection of oil spills and measurement of oil slicks using FOSPR sensors are expected to provide timely marine pollution prevention to minimize the threat to marine ecosystems.

MATERIALS AND METHODS

Materials

Sodium citrate, $NaBH_4$, gold (III) chloride trihydrate ($HAuCl_4 \cdot 3H_2O$), and dopamine hydrochloride were purchased from Aladdin Industrial Corporation (99% purity) (Shanghai, China). Hydroxylamine hydrochloride ($NH_2OH \cdot HCl$) was purchased from Sigma-Aldrich (St. Louis, MO, United States). All reagents used in this experiment were commercially available analytical grade. The oil used in our study was a light crude oil from China National Petroleum Corporation. Multimode fibers with a core diameter of 400 μm and an aperture of 0.22 were purchased from Ocean Optics, Inc. (United States).

FIGURE 1 | Schematic diagram of oil slick thickness measurements by fiber-optic surface plasmon resonance (FOSPR) sensor.

Fabrication of the Fiber-Optic Surface Plasmon Resonance Sensor

The cladding was stripped at one end of the multimode optical fiber using chemical methods to expose the fiber core. Then, the end face of the fiber core was polished (a photograph of the FOSPR sensor for oil detection is presented in **Supplementary Material**). PDA coating is a universal material for optical fiber functionalization by dopamine self-polymerization. In this study, the gold-film fiber sensor was fabricated by PDA-accelerated ELP, which we reported in previous study (Shi et al., 2016). In brief, the piranha solution was employed to clean the bare fiber for 30 min at 90°C, and then, the cleaned optical fiber was immersed in a dopamine solution at 10°C for 15 min. The PDA functionalized fiber adsorbed the gold seeds *via* immersion in colloidal gold solution for 2 h, which was synthesized by sodium citrate, $NaBH_4$, and gold (III) chloride trihydrate. Finally, the gold film was generated on the optical fiber by immersing the gold seed fiber in a solution with a mixture of 0.1 wt% gold (III) chloride trihydrate and 0.4 mM hydroxylamine hydrochloride and shaking for 5 min 30 s. The thin silver layer was coated onto the end surface of the gold film-coated fiber by a silver mirror reaction using Tollens' reagent. The resulting silver mirror is an essential component of the FOSPR sensor, which is responsible for the back reflection of the light in the fiber.

Fiber-Optic Surface Plasmon Resonance Sensor Set Up

A diagram of the sensor measurement system is shown in **Figure 1** and **Supplementary Figure 1**. A tungsten-halogen light source (DH-2000-BAL, Ocean Optics, Inc.) was used to provide stable UV-visible light at wavelengths between 200 and 1,000 nm. In our study, we employed 360–1,000 nm halogen light,

which entered the FOSPR sensor through a Y-type optical fiber (SPLIT-400-VIS-NIR, Ocean Optics, Inc.) (Tang et al., 2020). The sensing-region end of the FOSPR sensor was immersed in the solution to be measured. After SPR occurred under the excitation of the incident light, the signal was transmitted to the spectrometer (USB2000+, Ocean Optics, Inc.) through the other side of the Y-type optical fiber. The signal was displayed and monitored by a computer connected to the spectrometer (Shi et al., 2015). The thickness of the light crude oil film was detected using the fabricated FOSPR sensor, and the linear relationship between the intensity and thickness of the light crude oil film was calculated.

Detection of Oil Spill

As illustrated in **Figure 1**, the proposed FOSPR sensors can be set up near the oil spill point in the sea. Significant changes in light intensity and resonance wavelength can be observed, which arise from the differences in refraction between oil and water/air. Research has demonstrated that spectral differences can be used to research the relationship between thickness and specific wavelengths (Jiang et al., 2018), where wavelengths in the visible and near-infrared range are related to the oil slick thickness. We employed a wavelength range of 500–1,000 nm to study the reflectance change of oil slick thickness in the wavelength range. It was also found that different oil thicknesses led to changes in reflection spectra.

Oil slick thickness was examined at the water-oil, air-oil, and air-liquid interfaces, respectively (**Supplementary Figure 1**). Then, the thickness measurement of crude oil was carried out, in which crude oil with different volumes was added to the water surface (Jiang et al., 2018). We used a pipette to accurately measure the volume of crude oil and calculated the thickness h of

oil from the volume of crude oil on container S (the bottom area of the container used was 20 cm^2):

$$h = V/S$$

The total length of the sensing region was 10 mm, where the silver end was placed at the bottom of the sensor to enhance reflection. According to **Supplementary Figure 1**, an elevator platform was used to precisely control the height of the sensor. The sensing region was completely immersed in water at the water-oil interface. It was necessary to add a certain amount of oil and raise the fiber-optic sensor upward to keep the top of the sensor on the water-oil interface. The sensing region was exposed to the air while the silver end of the sensor was in the water at the air-oil interface. Thickness estimation at the water-oil and air-oil interfaces was carried out by adding a certain amount of oil to reach a thickness ranging from 0 to 10 mm. At the air-water interface, half of the sensing region was immersed in water, and the other was in the air to determine the minimum thickness that our SPR sensor could measure. We also investigated the effects of temperature and salinity, which are common factors in oil thickness monitoring, on the FOSPR sensor response.

RESULTS

Principles of Oil Detection

Surface plasmon resonance occurs at the sensing region covered with a metal nanofilm when white light is continuously conducted with total reflection in the optical fiber and transmitted from one end to the optical fiber sensing region (McDonagh et al., 2008). As the refractive index changes in the surrounding environment arising from oil spillage, the SPR spectra also change, and the entire sensing region of the FOSPR sensor provides a detection function (Wolfbeis, 2008). The measurement of oil thickness is implemented by detecting the interfaces between different liquid layers (air-oil and oil-water).

Measurement of Oil Slick Thickness

Thickness estimation at the water-oil interface was carried out by adding oil to reach a thickness ranging from 0 to 10 mm. While adding a certain amount of petroleum, the FOSPR sensor was raised upward to keep it at the top of the sensing region at the air-oil interface (**Figure 2A**). As shown in **Figure 2B**, the reflectance of oil declines at the oil-water interface as visible thickness increases from 500 to 1,000 nm, which is in line with previous research on the spectral responses of offshore oil slicks (Lu et al., 2008, 2013). Based on the reflection spectrum corresponding to the wavelength of 682.91 nm, the oil slick thickness is linearly fitted to obtain a linear relationship with a measurement coefficient R^2 of 0.955, as shown in **Figure 2C**.

Thickness detection at the air-oil interface was carried out by adding oil to reach a thickness range of 0–5 mm. As illustrated in **Figure 3A**, at the air-oil interface, the silver end is immersed in the water, and the sensing region remains in the air. The optical fiber sensor is used to measure the oil slick thickness in the air. **Figure 3B** shows that the reflectance spectrum gradually decreases as the oil slick thickness increases, and the coefficient R^2 is 0.998. High correlations are observed between oil spill spectral reflectance values and oil spill thickness measurements. The thick oil slick is characterized by low reflection, low penetrability, and strong absorption of incident visible light (Kingston, 2002).

Effects of Salinity and Temperature

Different salinities (25–45%) were used to determine the influence of ocean salinity fluctuations on oil thickness estimation according to the average salinity of the seawater, which was 35%. The temperature range of water and oil was 20–40°C. As illustrated in **Figure 4**, the spectrogram does not change significantly as the salinity and temperature increase. This indicates that changes in salinity and temperature (whether water or oil) have less effect on the measurement of oil slick thickness by the proposed sensor.
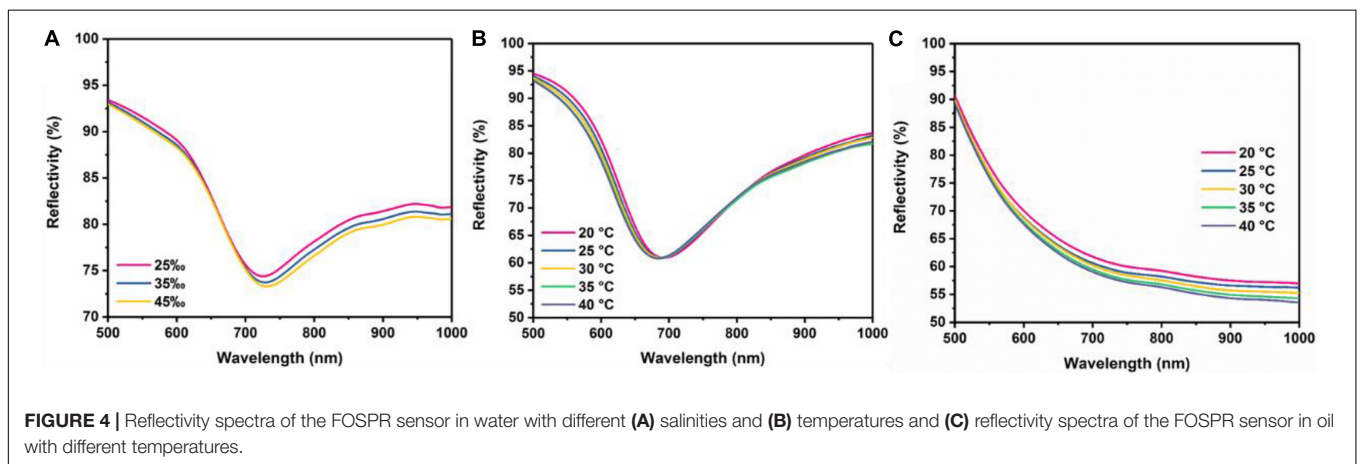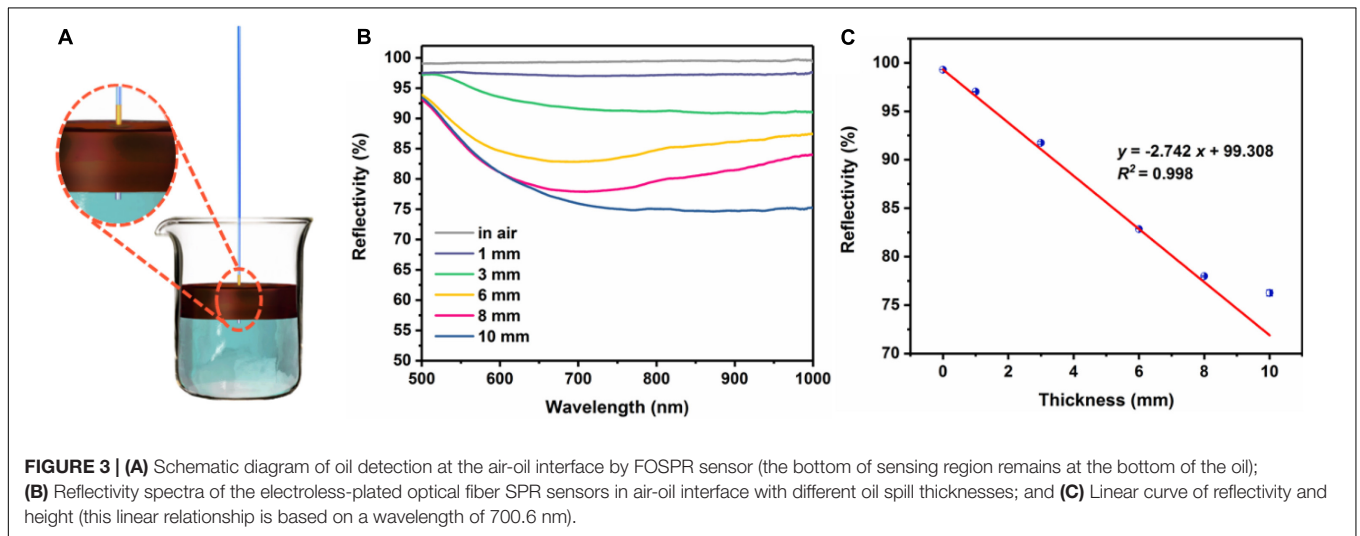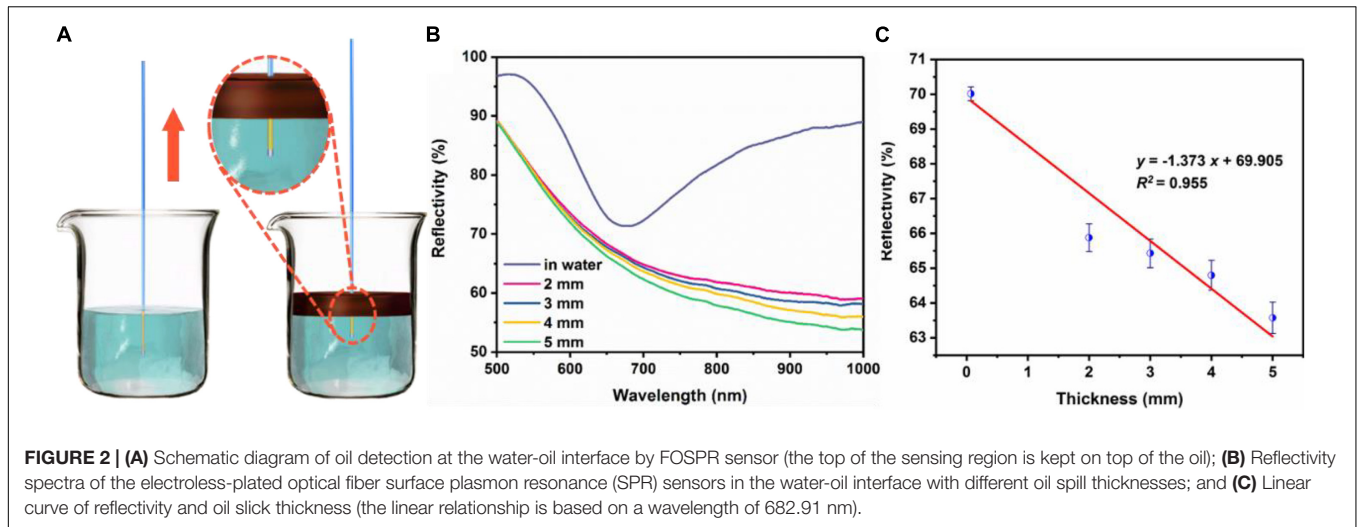
Repeatability

To explore the reusability of the optical fiber sensor after oil thickness measurement, the used FOSPR sensor was cleaned with water and detergent, followed by ozone treatment. In detail, the sensing regions of optical fiber were soaked in ultrapure water filled with detergent for approximately 10 min and then treated by ozone for 2 h (**Figure 5A**). As shown in **Figure 5B**, the spectrum of the sensor after cleaning returns to the resonance wavelength position before oil detection at a certain degree.

To determine the sensitivity of the as-cleaned sensor to the surrounding refractive index, the sensor was immersed in a series of different mass concentrations of sucrose solutions of varying refractive indices, ranging from 1.33 to 1.40. Then, a comparison experiment was conducted by immersing the optical fiber SPR sensor and cleaning sensor into the different concentrations of glucose solution. As shown in **Figure 5C**, the SPR wavelength redshifts with an increase in the refractive index. The blue line in **Figure 5D** indicates that the sensitivity of the cleaning sensor is 2,263 nm/RIU, which is lower than the red line, which has a sensitivity of 2,640 nm/RIU. The results show that the sensor after exposure to petroleum can still be used for detection, with a slight decrease in the sensitivity.
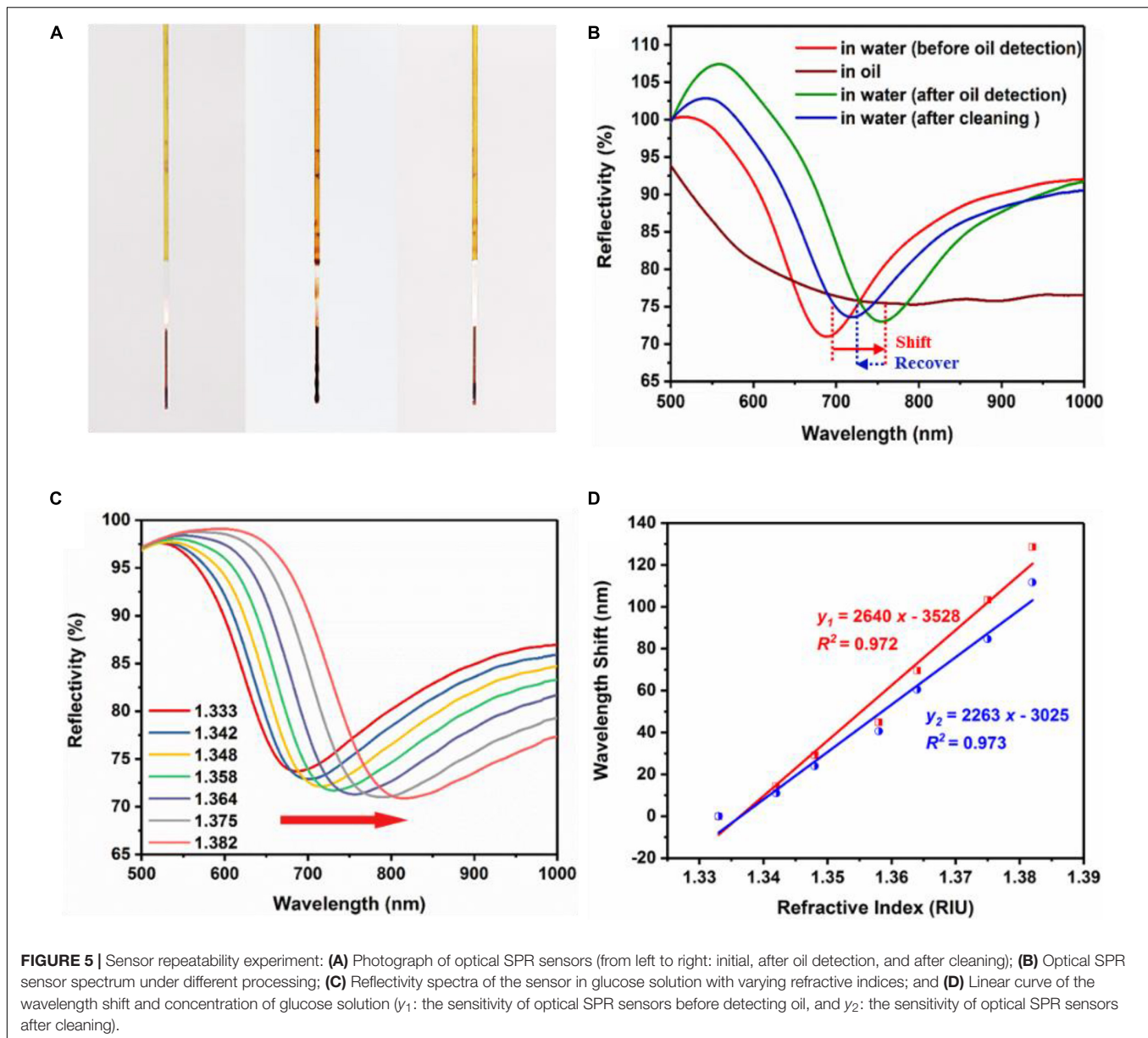
DISCUSSION

The thickness of oil is usually correlated to its visual appearance and color. Several measurement methods, such as microwave radiometry, laser fluorescence, and thermal sensors, have been applied to detect oil spills, and their advantages and disadvantages were summarized in **Supplementary Table 1**. Among these, microwave sensors have been used for a long time as indicators of oil slick thickness as the microwave brightness of slicks varies in a cyclical fashion with the thickness. Unfortunately, microwave brightness is also influenced by a number of other factors, such as weather, sea conditions, and the type of oil. Comparatively, fabricated fiber-optic SPR sensors show significant promise for detecting oil thickness, with real-time capabilities, high flexibility, corrosion resistance, and low cost. The high salt

FIGURE 2 | (A) Schematic diagram of oil detection at the water-oil interface by FOSPR sensor (the top of the sensing region is kept on top of the oil); **(B)** Reflectivity spectra of the electroless-plated optical fiber surface plasmon resonance (SPR) sensors in the water-oil interface with different oil spill thicknesses; and **(C)** Linear curve of reflectivity and oil slick thickness (the linear relationship is based on a wavelength of 682.91 nm).

FIGURE 3 | (A) Schematic diagram of oil detection at the air-oil interface by FOSPR sensor (the bottom of sensing region remains at the bottom of the oil); **(B)** Reflectivity spectra of the electroless-plated optical fiber SPR sensors in air-oil interface with different oil spill thicknesses; and **(C)** Linear curve of reflectivity and height (this linear relationship is based on a wavelength of 700.6 nm).

FIGURE 4 | Reflectivity spectra of the FOSPR sensor in water with different **(A)** salinities and **(B)** temperatures and **(C)** reflectivity spectra of the FOSPR sensor in oil with different temperatures.

concentration in most marine environments combined with high electrical conductivity makes marine bodies a highly conducive environment for corrosion to occur on metal surfaces, including iron and zinc. However, as the optical fiber SPR sensor is made of glass and has a gold layer with corrosion resistance, it does not encounter this problem.

FIGURE 5 | Sensor repeatability experiment: **(A)** Photograph of optical SPR sensors (from left to right: initial, after oil detection, and after cleaning); **(B)** Optical SPR sensor spectrum under different processing; **(C)** Reflectivity spectra of the sensor in glucose solution with varying refractive indices; and **(D)** Linear curve of the wavelength shift and concentration of glucose solution (y_1: the sensitivity of optical SPR sensors before detecting oil, and y_2: the sensitivity of optical SPR sensors after cleaning).

We simulated two situations of offshore oil spills in this study. The FOSPR sensor was immersed in water or oil and detected at two interfaces (water-oil and air-oil). In the construction of the entire optical fiber detection system, a fishing float was employed to ensure that the sensing area of the optical fiber sensor was perpendicular to the sea surface. The sensor responded quickly when oil drops appeared on the surface, and the sensing signal was transmitted to a computer and reflected by changes in light intensity and resonance wavelength. The measurement sensitivity of oil thickness at the air-oil interface was higher than at the water-oil interface, which could be due to the greater refractive index difference between air and oil compared with that of water and oil.

As displayed in **Figures 2**, **3**, we can see that the sensor responded effectively when it came into contact with oil. A linear curve of reflectivity and oil slick thickness was obtained using a fixed wavelength. The linear relationships were based on a wavelength of 682.91 nm for water-oil and a wavelength of 700.6 nm for air-oil, respectively. The reflectance corresponding to the wavelength of 700.6 nm at the air-oil interface could be determined from the detection reflection spectrogram of the spilled oil. Thus, oil thickness in different conditions could be calculated based on the relationship curve between thickness and reflectivity.

CONCLUSION

We proposed an optical fiber SPR sensor for the rapid measurement of oil slick thickness in this study. Two oil thickness measurement methods under different interfaces were presented. The measurement results at the water-oil interface showed that

the sensor had a high sensitivity of -1.373%/mm in the thickness range of 0–5 mm; at the air-oil interface, the sensor presented a sensitivity of -2.742%/mm in the thickness range of 0–10 mm. Experimental results also indicated that salinity and temperature changes had less influence on oil thickness measurement, and the FOSPR sensor had good repeatability. The unique advantages of optical fiber have significant application prospects for use in marine oil spill detection and thickness measurements, such as miniaturization, high flexibility, corrosion resistance, and anti-interference. The proposed FOSPR sensor has great potential for submarine oil spill detection at the water-oil interface.

DATA AVAILABILITY STATEMENT

The original contributions presented in the study are included in the article/**Supplementary Material**, further inquiries can be directed to the corresponding author.

AUTHOR CONTRIBUTIONS

HY, JL, and RS designed the research. HY, SC, and RS conducted the analysis. All authors contributed to writing and editing the manuscript.

FUNDING

SUPPLEMENTARY MATERIAL

The Supplementary Material for this article can be found online at: https://www.frontiersin.org/articles/10.3389/fmars.2021.764970/full#supplementary-material

REFERENCES

Beyer, J., Trannum, H. C., Bakke, T., Hodson, P. V., and Collier, T. K. (2016). Environmental effects of the deepwater horizon oil spill: a review. *Mar. Pollut. Bull.* 110, 28–51. doi: 10.1016/j.marpolbul.2016.06.027

Brown, C. E., and Fingas, M. F. (2003). Development of airborne oil thickness measurements. *Mar. Pollut. Bull.* 47, 485–492. doi: 10.1016/s0025-326x(03)00203-0

Bukin, O., Proschenko, D., Alexey, C., Korovetskiy, D., Bukin, I., Yurchik, V., et al. (2020). New solutions of laser-induced fluorescence for oil pollution monitoring at sea. *Photonics* 7:36. doi: 10.3390/photonics7020036

Caillault, K., Roupioz, L., and Viallefont-Robinet, F. (2021). Modelling of the optical signature of oil slicks at sea for the analysis of multi- and hyperspectral VNIR-SWIR images. *Opt. Express* 29, 18224–18242. doi: 10.1364/OE.424953

De Padova, D., Mossa, M., Adamo, M., De Carolis, G., and Pasquariello, G. (2017). Synergistic use of an oil drift model and remote sensing observations for oil spill monitoring. *Environ. Sci. Pollut. Res.* 24, 5530–5543. doi: 10.1007/s11356-016-8214-8

Fingas, M. (2018). The challenges of remotely measuring oil slick thickness. *Remote Sens.* 10:28. doi: 10.3390/rs10020319

Fingas, M., and Brown, C. (2014). Review of oil spill remote sensing. *Mar. Pollut. Bull.* 83, 9–23. doi: 10.1016/j.marpolbul.2014.03.059

Garcia-Pineda, O., Staples, G., Jones, C. E., Hu, C. M., Holt, B., Kourafalou, V., et al. (2020). Classification of oil spill by thicknesses using multiple remote sensors. *Remote Sens. Environ.* 236:111421. doi: 10.1016/j.rse.2019.111421

Goswami, N., Chauhan, K. K., and Saha, A. (2016). Analysis of surface plasmon resonance based bimetal coated tapered fiber optic sensor with enhanced sensitivity through radially polarized light. *Opt. Commun.* 379, 6–12. doi: 10.1016/j.optcom.2016.05.047

Guo, G., Liu, B. X., and Liu, C. Y. (2020). Thermal infrared spectral characteristics of bunker fuel oil to determine oil-film thickness and API. *J. Mar. Sci. Eng.* 8:135. doi: 10.3390/jmse8020135

Hoseinian, M. S., and Bolorizadeh, M. A. (2019). Design and simulation of a highly sensitive SPR optical fiber sensor. *Photonic Sens.* 9, 33–42. doi: 10.1007/s13320-018-0508-7

Jiang, W. T., Li, J. W., Yao, X. L., Forsberg, E., and He, S. L. (2018). Fluorescence hyperspectral imaging of oil samples and its quantitative applications in component analysis and thickness estimation. *Sensors* 18:4415. doi: 10.3390/s18124415

Jiao, J. N., Lu, Y. C., Hu, C. A. M., Shi, J., Sun, S. J., and Liu, Y. X. (2021). Quantifying ocean surface oil thickness using thermal remote sensing. *Remote Sens. Environ.* 261:112513. doi: 10.1016/j.rse.2021.112513

Kingston, P. F. (2002). Long-term environmental impact of oil spills. *Spill Sci. Technol. Bull.* 7, 53–61. doi: 10.1016/s1353-2561(02)00051-8

Leifer, I., Lehr, W. J., Simecek-Beatty, D., Bradley, E., Clark, R., Dennison, P., et al. (2012). State of the art satellite and airborne marine oil spill remote sensing: application to the BP deepwater horizon oil spill. *Remote Sens. Environ.* 124, 185–209. doi: 10.1016/j.rse.2012.03.024

Li, G. N., Li, Y., Hou, Y. C., Wang, X., and Wang, L. (2021). Marine oil slick detection using improved polarimetric feature parameters based on polarimetric synthetic aperture radar data. *Remote Sens.* 13:1607. doi: 10.3390/rs13091607

Li, Y., Liu, B.-X., Li, B.-Y., and Chen, D. (2012). Analysis of spectral characteristics of oil film on water based on wavelet transform. *Spectrosc. Spectral Anal.* 32, 1923–1927. doi: 10.3964/j.issn.1000-0593201207-1923-05

Liu, Z., Liu, L., Zhu, Z., Zhang, Y., Wei, Y., Zhang, Y., et al. (2017). Dual-channel surface plasmon resonance refractive index sensor based on modified hetero-core structure fiber. *Opt. Commun.* 403, 290–295. doi: 10.1016/j.optcom.2017.07.064

Lu, Y., Tian, Q., Wang, J., Wang, X., and Qi, X. (2008). Experimental study on spectral responses of offshore oil slick. *Chin. Sci. Bull.* 53, 3937–3941. doi: 10.1007/s11434-008-0515-y

Lu, Y. C., Tian, Q. J., Wang, X. Y., Zheng, G., and Li, X. (2013). Determining oil slick thickness using hyperspectral remote sensing in the Bohai Sea of China. *Int. J. Digital Earth* 6, 76–93. doi: 10.1080/17538947.2012.695404

Massaro, A., Lay-Ekuakille, A., Caratelli, D., Palamara, I., and Morabito, F. C. (2012). Optical performance evaluation of oil spill detection methods: thickness and extent. *IEEE Trans. Instrum. Meas.* 61, 3332–3339. doi: 10.1109/tim.2012.2210336

McDonagh, C., Burke, C. S., and MacCraith, B. D. (2008). Optical chemical sensors. *Chem. Rev.* 108, 400–422. doi: 10.1021/cr068102g

Miliutina, E., Kalachyova, Y., Postnikov, P., Svorcik, V., and Lyutakov, O. (2020). Enhancement of surface plasmon fiber sensor sensitivity through the grafting of gold nanoparticles. *Photonic Sens.* 10, 105–112. doi: 10.1007/s13320-019-0562-9

Moon, J., and Jung, M. (2020). Geometrical properties of spilled oil on seawater detected using a LiDAR sensor. *J. Sens.* 2020:5609168. doi: 10.1155/2020/5609168

Naz, S., Iqbal, M. F., Mahmood, I., and Allam, M. (2021). Marine oil spill detection using Synthetic Aperture Radar over Indian Ocean. *Mar. Pollut. Bull.* 162, 111921–111921. doi: 10.1016/j.marpolbul.2020.111921

Patnaik, A., Senthilnathan, K., and Jha, R. (2015). Graphene-based conducting metal oxide coated D-shaped optical fiber SPR sensor. *IEEE Photonics Technol. Lett.* 27, 2437–2440. doi: 10.1109/lpt.2015.2467189

Peterson, C. H., Rice, S. D., Short, J. W., Esler, D., Bodkin, J. L., Ballachey, B. E., et al. (2003). Long-term ecosystem response to the Exxon Valdez oil spill. *Science* 302, 2082–2086. doi: 10.1126/science.1084282

Rotkin-Ellman, M., Navarro, K. M., and Solomon, G. M. (2010). Gulf oil spill air quality monitoring: lessons learned to improve emergency response. *Environ. Sci. Technol.* 44, 8365–8366. doi: 10.1021/es103323v

Saleh, M., Oueidat, G., Elhajj, I. H., and Asmar, D. (2019). In situ measurement of oil slick thickness. *IEEE Trans. Instrum. Meas.* 68, 2635–2647. doi: 10.1109/tim.2018.2866745

Schaum, J., Cohen, M., Perry, S., Artz, R., Draxler, R., Frithsen, J. B., et al. (2010). Screening level assessment of risks due to dioxin emissions from burning oil from the BP deepwater horizon Gulf of Mexico spill. *Environ. Sci. Technol.* 44, 9383–9389. doi: 10.1021/es103559w

Semwal, V., Shrivastav, A. M., Verma, R., and Gupta, B. D. (2016). Surface plasmon resonance based fiber optic ethanol sensor using layers of silver/silicon/hydrogel entrapped with ADH/NAD. *Sens. Actuators B Chem.* 230, 485–492. doi: 10.1016/j.snb.2016.02.084

Sharma, A. K., Jha, R., and Gupta, B. D. (2007). Fiber-optic sensors based on surface plasmon resonance: a comprehensive review. *IEEE Sens. J.* 7, 1118–1129. doi: 10.1109/jsen.2007.897946

Shi, S., Wang, L. B., Su, R. X., Liu, B. S., Huang, R. L., Qi, W., et al. (2015). A polydopamine-modified optical fiber SPR biosensor using electroless-plated gold films for immunoassays. *Biosens. Bioelectron.* 74, 454–460. doi: 10.1016/j.bios.2015.06.080

Shi, S., Wang, L. B., Wang, A. K., Huang, R. L., Ding, L., Su, R. X., et al. (2016). Bioinspired fabrication of optical fiber SPR sensors for immunoassays using polydopamine-accelerated electroless plating. *J. Mater. Chem. C* 4, 7554–7562. doi: 10.1039/c6tc02149b

Shih, W.-C., and Andrews, A. B. (2008). Modeling of thickness dependent infrared radiance contrast of native and crude oil covered water surfaces. *Opt. Express* 16, 10535–10542. doi: 10.1364/oe.16.010535

Shrivastav, A. M., Usha, S. P., and Gupta, B. D. (2016). Fiber optic profenofos sensor based on surface plasmon resonance technique and molecular imprinting. *Biosens. Bioelectron.* 79, 150–157. doi: 10.1016/j.bios.2015.11.095

Sun, S. J., and Hu, C. M. (2019). The challenges of interpreting oil-water spatial and spectral contrasts for the estimation of oil thickness: examples from satellite and airborne measurements of the deepwater horizon oil spill. *IEEE Trans. Geosci. Electron.* 57, 2643–2658. doi: 10.1109/tgrs.2018.2876091

Tang, Y. W., Yuan, H., Chen, J. P., Xing, Q. G., Su, R. X., Qi, W., et al. (2020). Polydopamine-assisted fabrication of stable silver nanoparticles on optical fiber for enhanced plasmonic sensing. *Photonic Sens.* 10, 97–104. doi: 10.1007/s13320-019-0564-7

Tong, S., Liu, X., Chen, Q., Zhang, Z., and Xie, G. (2019). Multi-feature based ocean oil spill detection for polarimetric SAR data using random forest and the self-similarity parameter. *Remote Sens.* 11:451. doi: 10.3390/rs11040451

Wan, Z., and Chen, J. H. (2018). Human errors are behind most oil-tanker spills. *Nature* 560, 161–163. doi: 10.1038/d41586-018-05852-0

Washburn, T. W., Yoskowitz, D. W., and Montagna, P. A. (2018). Valuing nature waste removal in the offshore environment following the deepwater horizon oil spill. *Front. Mar. Sci.* 5:477. doi: 10.3389/fmars.2018.00477

Wettle, M., Daniel, P. J., Logan, G. A., and Thankappan, M. (2009). Assessing the effect of hydrocarbon oil type and thickness on a remote sensing signal: a sensitivity study based on the optical properties of two different oil types and the HYMAP and Quickbird sensors. *Remote Sens. Environ.* 113, 2000–2010. doi: 10.1016/j.rse.2009.05.010

Wolfbeis, O. S. (2008). Fiber-optic chemical sensors and biosensors. *Anal. Chem.* 80, 4269–4283. doi: 10.1021/ac800473b

Ye, Z., Liu, L., We, C. X., Qun, G., An, P. A., Zhao, Y. J., et al. (2015). Experimental methods and result analysis of a variety of spectral reflectance properties of the thin oil film. *Spectrosc. Spectral Anal.* 35, 1695–1699. doi: 10.3964/j.issn.1000-0593201506-1695-05

Zhan, Y., Mao, T., Gong, F., Wang, D., and Chen, J. (2010). "An oil film information retrieval method overcoming the influence of sun glitter - based on AISA plus airborne hyper-spectral image," in *Proceedings of the Remote Sensing of the Ocean, Sea Ice, and Large Water Regions 2010*, eds C. R. Bostater, S. P. Mertikas, X. Neyt, and M. VelezReyes (Bellingham, WA: SPIE).

Zhao, C. L., Wang, Y. R., Wang, D. N., and Ding, Z. W. (2017). Numerical investigation into a surface plasmon resonance sensor based on optical fiber microring. *Photonic Sens.* 7, 105–112. doi: 10.1007/s13320-017-0359-7